Chiral Magnetic Effect and QCD Phase Transitions with Effective Models

Wei-jie Fu,[1,*] Yu-xin Liu,[2,3,†] and Yue-liang Wu[1,‡]

[1]*Kavli Institute for Theoretical Physics China (KITPC),*
Key Laboratory of Frontiers in Theoretical Physics, Institute of Theoretical Physics,
Chinese Academy of Science, Beijing 100190, China

[2]*Department of Physics and State Key Laboratory of Nuclear Physics and Technology,*
Peking University, Beijing 100871, China

[3]*Center of Theoretical Nuclear Physics,*
National Laboratory of Heavy Ion Accelerator, Lanzhou 730000, China

(Dated: March 23, 2010)

Abstract

We study the influence of the chiral phase transition on the chiral magnetic effect. The chiral electric current density along the magnetic field, the electric charge difference between on each side of the reaction plane, and the azimuthal charged-particle correlations as functions of the temperature during the QCD phase transitions are calculated. It is found that with the decrease of the temperature, the chiral electric current density, the electric charge difference, and the azimuthal charged-particle correlations all get a sudden suppression at the critical temperature of the chiral phase transition, because the large quark constituent mass in the chiral symmetry broken phase quite suppresses the axial anomaly and the chiral magnetic effect. We suggest that the azimuthal charged-particle correlations (including the correlators divided by the total multiplicity of produced charged particles which are used in current experiments and another kind of correlators not divided by the total multiplicity) can be employed to identify the occurrence of the QCD phase transitions in RHIC energy scan experiments.

PACS numbers: 25.75.Nq 11.30.Er, 11.30.Rd, 11.30.Qc,

*wjfu@itp.ac.cn
†yxliu@pku.edu.cn
‡ylwu@itp.ac.cn

I. INTRODUCTION

The phase transitions of quantum chromodynamics (QCD), for example the phase transition of the chiral symmetry restoration and the deconfinement phase transition, have attracted lots of attentions in recent years. It is expected that these phase transitions occur and the deconfined quark gluon plasma (QGP) is formed in ultrarelativistic heavy-ion collisions [1–5] (for example the current experiments at the Relativistic Heavy Ion Collider (RHIC) and the Large Hadron Collider (LHC)) and in the interior of neutron stars [6–8]. Furthermore, studying the QCD phase transitions is also an elementary problem in strong interaction physics.

Recently, The STAR Collaboration at RHIC report their measurements of azimuthal charged-particle correlations near center-of-mass rapidity in Au + Au and Cu + Cu collisions at $\sqrt{s_{NN}} = 200\,\mathrm{GeV}$. They find a significant signal consistent with the charge separation of quarks along the system's orbital angular momentum axis [9, 10]. The observed charge separation indicates that parity-odd domains, where the parity ($\mathcal{P}$) symmetry is locally violated, might be created during the relativistic heavy-ion collisions [11, 12].

QCD is an SU(3) Yang-Mills gauge theory coupled with quarks. The gauge field can have nontrivial configurations which can be characterized by a topological invariant, the winding number Q_w [13]. The winding number is an integer and reads $Q_w = \frac{g^2}{32\pi^2}\int d^4x G^a_{\mu\nu}\tilde{G}^{\mu\nu}_a$. Here g is the QCD coupling constant. The gluon field tensor and its dual are $G^a_{\mu\nu}$ and $\tilde{G}^{\mu\nu}_a = \frac{1}{2}\epsilon^{\mu\nu\rho\sigma}G^a_{\rho\sigma}$. The nontrivial gauge field configurations with non-zero winding number Q_w can result in non-conservation of the axial currents due to the axial anomaly [14], i.e.,

$$\partial^\mu j^5_\mu = 2\sum_f m_f\langle\bar{\psi}_f i\gamma_5\psi_f\rangle_A - \frac{N_f g^2}{16\pi^2}G^a_{\mu\nu}\tilde{G}^{\mu\nu}_a, \tag{1}$$

where ψ_f is a quark field, m_f is the current mass of the quark, and N_f is the number of quark flavors. $j^5_\mu = \sum_f\langle\bar{\psi}_f\gamma_\mu\gamma_5\psi_f\rangle_A$ denotes the axial current density in the background of a gauge field configuration A^a_μ. Integrating the two sides of Eq. (1) over three dimension space and one dimension time and assuming the number of right-handed and left-handed fermions is equal initially at $t = -\infty$, we obtain

$$(N_R - N_L)_{t=\infty} = -2N_f Q_w. \tag{2}$$

From Eq. (2) one can clearly find that through the interactions between quarks and nontrivial gluon configuration with non-zero Q_w, the right-handed quarks are converted into

left-handed quarks, vice versa depending on the sign of the winding number. Then there will be an asymmetry between the number of right- and left-handed quarks. When a magnetic field is added, an electric current is induced along the magnetic field and positive charges are separated from negative charge, which is called the "chiral magnetic effect" [15–20].

Now that the chiral magnetic effect can be observed through the measurements of azimuthal charged-particle correlations in the relativistic heavy-ion collisions, a natural question arises, i.e. whether can we detect the properties of the QCD phase transitions, especially the chiral phase transition through the observations of the chiral magnetic effect? To answer this question, we have to study how the chiral magnetic effect or the charge separation effect is influenced by the chiral phase transition. This is our central subject in this work.

This work is the extension of our former work [21] and presents many details. The paper is organized as follows. In Sec. II we simply introduce the thermodynamics of the 2+1 flavor Polyakov–Nambu–Jona-Lasinio (PNJL) model. In Sec. III we will calculate the chiral electric current density along the direction of the magnetic field and study its dependence on the temperature during the QCD phase transitions. In Sec. IV we will calculate the electric difference between on each side of the reaction plane and the azimuthal charged-particle correlations in heavy ion collisions. In Sec. V we present our summary and conclusions.

II. THERMODYNAMICS OF 2+1 FLAVOR PNJL MODEL

In this work, we will study the chiral magnetic effect and the QCD phase transitions in the 2+1 flavor Polyakov–Nambu–Jona-Lasinio model. The validity of the PNJL model has been confirmed in a series of works by confronting the PNJL results with the lattice QCD data [22–26]. The PNJL model not only has the chiral symmetry and the dynamical breaking mechanism of this symmetry, which are same as the conventional Nambu–Jona-Lasinio model, but also include the effect of color confinement through the Polyakov loop. Therefore, the PNJL model is very appropriate to describe the QCD phase transitions at finite temperature and/or density.

In this work, we employ the 2+1 flavor Polyakov-loop improved NJL model which has been discussed in details in our previous work [25], and the Lagrangian density for the 2+1

flavor PNJL model is given as

$$
\begin{aligned}
\mathcal{L}_{\rm PNJL} \ = \ & \bar{\psi}(i\gamma_\mu D^\mu - \hat{m}_0)\psi + G\sum_{a=0}^{8}\Big[(\bar{\psi}\tau_a\psi)^2 \\
& +(\bar{\psi}i\gamma_5\tau_a\psi)^2\Big] - K\Big[\det{}_f\big(\bar{\psi}(1+\gamma_5)\psi\big) \\
& +\det{}_f\big(\bar{\psi}(1-\gamma_5)\psi\big)\Big] - \mathcal{U}(\Phi,\Phi^*,T), \qquad (3)
\end{aligned}
$$

where $\psi = (\psi_u, \psi_d, \psi_s)^T$ is the three-flavor quark field,

$$
D^\mu = \partial^\mu - iA^\mu \quad \text{with} \quad A^\mu = \delta^\mu_0 A^0 \quad , \quad A^0 = g\mathcal{A}^0_a \frac{\lambda_a}{2} = -iA_4. \qquad (4)
$$

λ_a are the Gell-Mann matrices in color space and the gauge coupling g is combined with the SU(3) gauge field $\mathcal{A}^\mu_a(x)$ to define $A^\mu(x)$ for convenience. $\hat{m}_0 = \mathrm{diag}(m_0^u, m_0^d, m_0^s)$ is the three-flavor current quark mass matrix. Throughout this work, we take $m_0^u = m_0^d \equiv m_0^l$, while keep m_0^s being larger than m_0^l, which breaks the $SU(3)_f$ symmetry. In the above PNJL Lagrangian, $\mathcal{U}\left(\Phi,\Phi^*,T\right)$ is the Polyakov-loop effective potential, which is expressed in terms of the traced Polyakov-loop $\Phi = (\mathrm{Tr}_c L)/N_c$ and its conjugate $\Phi^* = (\mathrm{Tr}_c L^\dagger)/N_c$ with the Polyakov-loop L being a matrix in color space given explicitly by

$$
L\left(\vec{x}\right) = \mathcal{P}\exp\left[i\int_0^\beta d\tau\, A_4\left(\vec{x},\tau\right)\right] = \exp\left[i\beta A_4\right] , \qquad (5)
$$

with $\beta = 1/T$ being the inverse of temperature and $A_4 = iA^0$.

In our work, we use the Polyakov-loop effective potential which is a polynomial in Φ and Φ^* [22], given by

$$
\frac{\mathcal{U}\left(\Phi,\Phi^*,T\right)}{T^4} = -\frac{b_2(T)}{2}\Phi^*\Phi - \frac{b_3}{6}(\Phi^3+\Phi^{*3}) + \frac{b_4}{4}(\Phi^*\Phi)^2 , \qquad (6)
$$

with

$$
b_2(T) = a_0 + a_1\left(\frac{T_0}{T}\right) + a_2\left(\frac{T_0}{T}\right)^2 + a_3\left(\frac{T_0}{T}\right)^3 . \qquad (7)
$$

Parameters in the effective potential are fitted to reproduce the thermodynamical behavior of the pure-gauge QCD obtained from the lattice simulations. Their values are $a_0 = 6.75$, $a_1 = -1.95$, $a_2 = 2.625$, $a_3 = -7.44$, $b_3 = 0.75$ and $b_4 = 7.5$. The parameter T_0 is the critical temperature for the deconfinement phase transition to take place in the pure-gauge QCD and T_0 is chosen to be 270 MeV according to the lattice calculations. Furthermore, we also need to determine the five parameters in the quark sector of the model, which are $m_0^l = 5.5$ MeV,

$m_0^s = 140.7$ MeV, $G\Lambda^2 = 1.835$, $K\Lambda^5 = 12.36$ and $\Lambda = 602.3$ MeV. They are fixed by fitting $m_\pi = 135.0$ MeV, $m_K = 497.7$ MeV, $m_{\eta'} = 957.8$ MeV and $f_\pi = 92.4$ MeV [27].

In the parity-odd domains which are created during relativistic heavy-ion collisions, the number of left- and right-hand quarks is different because of the axial anomaly. In this work we introduce the chiral chemical potential μ_5 to study the left-right asymmetry following the method of Ref. [15], where the chiral chemical potential μ_5 is related with the effective theta angle of the θ-vacuum through $\mu_5 = \partial_0\theta/2N_f$ and N_f is the number of flavor. Consequently, we should add the following term

$$\bar{\psi}\hat{\mu}_5\gamma^0\gamma^5\psi \tag{8}$$

to the Lagrangian density in Eq. (3), where $\hat{\mu}_5 = \mathrm{diag}(\mu_5^u, \mu_5^d, \mu_5^s)$. Next, we consider the case that a homogenous magnetic field B is along the direction of the orbital angular momentum of the system produced in a non-central heavy-ion collision. In the following we denote this direction with z-direction and particle momentum in this direction with p_3. We derive the corresponding thermodynamics for a system with only one kind of a fermion in detail in Appendix A. In the Appendixes, we have emphasized that the approach used in Appendix A is appropriate to describe the chiral magnetic effect, while the modified Lagrangian approach in Appendix B is inappropriate. The results in Appendix A can be easily generalized to the 2+1 flavor PNJL model and in the mean field approximation, the thermodynamical potential density ($\Omega = -(T/V)\ln Z$) for the 2+1 flavor quark system under a homogeneous

background magnetic field B and with left-right asymmetry is given by

$$\begin{aligned}\Omega = & -N_c \sum_{f=u,d,s} \frac{|q_f|eB}{2\pi} \sum_{n=0}^{\infty} \sum_{s=\pm 1} \int \frac{dp_3}{2\pi} \Big(E_f \\ & + \frac{T}{3} \ln \Big\{ 1 + 3\Phi^* \exp\big[- \big(E_f - \mu_f - \frac{s|\epsilon_f|}{E_f} \mu_5^f \big)/T \big] \\ & + 3\Phi \exp\big[- 2\big(E_f - \mu_f - \frac{s|\epsilon_f|}{E_f} \mu_5^f \big)/T \big] \\ & + \exp\big[- 3\big(E_f - \mu_f - \frac{s|\epsilon_f|}{E_f} \mu_5^f \big)/T \big] \Big\} + \frac{T}{3} \ln \Big\{ 1 \\ & + 3\Phi \exp\big[- \big(E_f + \mu_f - \frac{s|\epsilon_f|}{E_f} \mu_5^f \big)/T \big] \\ & + 3\Phi^* \exp\big[- 2\big(E_f + \mu_f - \frac{s|\epsilon_f|}{E_f} \mu_5^f \big)/T \big] \\ & + \exp\big[- 3\big(E_f + \mu_f - \frac{s|\epsilon_f|}{E_f} \mu_5^f \big)/T \big] \Big\} \Big) \\ & + 2G({\phi_u}^2 + {\phi_d}^2 + {\phi_s}^2) - 4K \phi_u \, \phi_d \, \phi_s \\ & + \mathcal{U}(\Phi, \Phi^*, T), \end{aligned} \tag{9}$$

where we have

$$|\epsilon_f| = \sqrt{2n|q_f|eB + p_3^2} \tag{10}$$

and

$$E_f = \sqrt{2n|q_f|eB + p_3^2 + M_f^2}. \tag{11}$$

Here $q_i (i = u, d, s)$ is the electric charge in unit of elementary charge e for the quark of flavor i. The constituent mass M_i is

$$M_i = m_0^i - 4G\phi_i + 2K\phi_j \, \phi_k, \tag{12}$$

and ϕ_i is the chiral condensate $\langle \bar{\psi}\psi \rangle_i$. We also include the quark chemical potential μ_i in Eq. (9). From our calculations in Appendix A, one can find that the momenta of charged particles in the longitudinal direction, i.e., the z-direction, are not influenced by the background magnetic field and p_3 in the expression of the thermodynamical potential density in Eq. (9) is continuous; while the momenta in the transverse plane are discretized due to the external magnetic field. We should emphasize that at the lowest order of the transverse quantum number $n = 0$, i.e., the lowest order Landau level, the quark spin only has one value in the z-direction, which means that charged particles in the lowest order Landau level

are polarized by the external magnetic field; however particles in higher levels, i.e., $n > 0$, are not polarized. Therefore, the charge separation effect only comes from quarks in the lowest order Landau level.

III. CHIRAL ELECTRIC CURRENT ALONG THE DIRECTION OF THE MAGNETIC FIELD

The chiral electric current along the longitudinal direction, i.e. the direction of the magnetic field, is an observable which describes the magnitude of the charge separation effect. Here, we use the approach in Appendix A to calculate the chiral electric current density j_3, whose expression is

$$\begin{aligned} j_3 &= \frac{e}{V}\int d^3x\bar{\psi}\hat{q}\gamma^3\psi \\ &= N_c\sum_{f=u,d,s}\frac{q_f^2e^2B}{4\pi^2}\Big[\int_0^\infty dp_3\frac{p_3}{E_f}f\big(E_f-\mu_f-\frac{p_3}{E_f}\mu_5^f\big) \\ &\quad -\int_0^\infty dp_3\frac{p_3}{E_f}f\big(E_f-\mu_f+\frac{p_3}{E_f}\mu_5^f\big)+\int_0^\infty dp_3\frac{p_3}{E_f}\bar{f}\big(E_f \\ &\quad +\mu_f-\frac{p_3}{E_f}\mu_5^f\big)-\int_0^\infty dp_3\frac{p_3}{E_f}\bar{f}\big(E_f+\mu_f+\frac{p_3}{E_f}\mu_5^f\big)\Big], \end{aligned} \tag{13}$$

where $\hat{q}e = \mathrm{diag}(q_ue, q_de, q_se)$ is the electric charge matrix for three-flavor quarks; V is the volume of the system and E_f is given by Eq. (11) with $n = 0$. We have

$$f(x) = \frac{\Phi^* e^{-x/T} + 2\Phi e^{-2x/T} + e^{-3x/T}}{1 + 3\Phi^* e^{-x/T} + 3\Phi e^{-2x/T} + e^{-3x/T}} \tag{14}$$

and

$$\bar{f}(x) = \frac{\Phi e^{-x/T} + 2\Phi^* e^{-2x/T} + e^{-3x/T}}{1 + 3\Phi e^{-x/T} + 3\Phi^* e^{-2x/T} + e^{-3x/T}}. \tag{15}$$

In order to study whether the chiral electric current is affected by the temperature, quark chemical potential, quark constituent mass and so on, we just pause here, and turn to the simpler system composed of only one type of fermion with positive charge e and mass m. The chiral electric current corresponding to this system is given by

$$\begin{aligned} j_3 &= \frac{e^2B}{4\pi^2}\Big[\int_0^\infty dp_3\frac{p_3}{E}\frac{1}{e^{(E-\mu-\frac{p_3}{E}\mu_5)/T}+1}-\int_0^\infty dp_3\frac{p_3}{E}\frac{1}{e^{(E-\mu+\frac{p_3}{E}\mu_5)/T}+1} \\ &\quad +\int_0^\infty dp_3\frac{p_3}{E}\frac{1}{e^{(E+\mu-\frac{p_3}{E}\mu_5)/T}+1}-\int_0^\infty dp_3\frac{p_3}{E}\frac{1}{e^{(E+\mu+\frac{p_3}{E}\mu_5)/T}+1}\Big]. \end{aligned} \tag{16}$$

where

$$E = \sqrt{p_3^2 + m^2}. \tag{17}$$

It is interesting to consider the case that fermions are massless, i.e., $m = 0$ in Eq. (17), then it can be easily obtained that

$$j_3 = \frac{e^2 B}{2\pi^2}\mu_5. \tag{18}$$

This is the result obtained in the modified Lagrangian approach as Eq. (B23) shows. However, the chiral electric current calculated in our approach is in essence different from that obtained in the modified Lagrangian approach. From our calculations above, one can find that the chiral electric current comes from the finite temperature part of the thermodynamics, i.e., from fermions and anti-fermions, whereas the electric current in the modified Lagrangian approach comes from the Dirac Sea, not from fermions and anti-fermions (for more details see Appendix B). Furthermore, although j_3 obtained in our approach only depends on the magnetic field strength B and the chiral chemical potential μ_5 in the massless case, it is indeed dependent on the temperature and the chemical potential μ when the mass of fermions is nonvanishing. On the contrary, j_3 in the modified approach only depends on B and μ_5, regardless of whether the mass of fermions is vanishing, which is due to the unphysical ultraviolet momentum in the Dirac Sea.

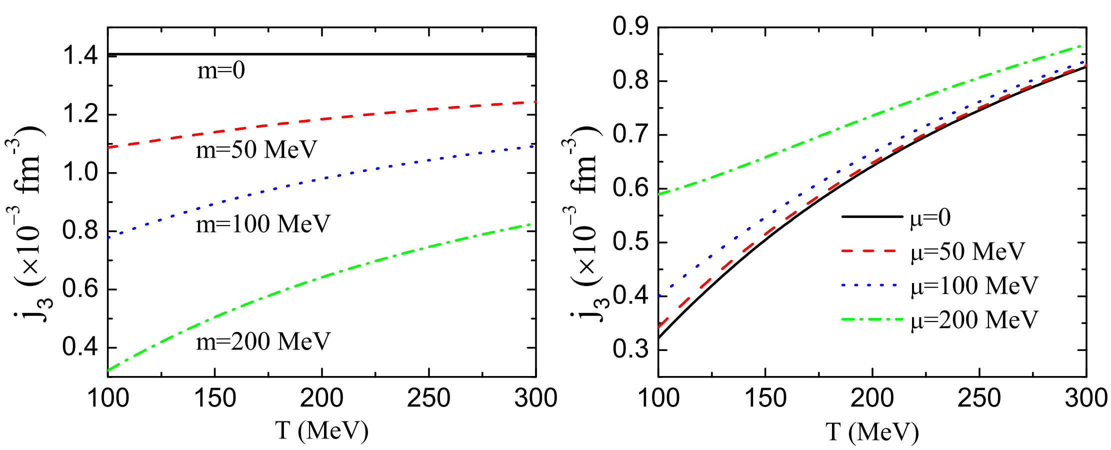

FIG. 1: (color online). Left panel: chiral electric current density j_3 in Eq. (16) as function of the temperature with several values of the fermion mass m, with $eB = 10^4\,\mathrm{MeV}^2$, $\mu = 0$, and $\mu_5 = 250\,\mathrm{MeV}$. Right panel: j_3 as function of the temperature with several values of the chemical potential μ and with $eB = 10^4\,\mathrm{MeV}^2$, $\mu_5 = 250\,\mathrm{MeV}$, and $m = 200\,\mathrm{MeV}$.

In order to verify our argument, we calculate the chiral electric current density in Eq. (16) for the one fermion system numerically, and the results are plotted in Fig. 1. From the figure one can easily find that, although the chiral electric current density is independent of the temperature when the fermion is massless as the black solid line in the left panel shows, it is indeed dependent of the temperature and the chemical potential in the case that the mass of fermion is nonvanishing. The effect of the mass of the electric current carrier, i.e., the fermion, is to decrease j_3, since the velocity of the fermion becomes smaller when the mass of the fermion is increased with a fixed energy. On the contrary, the chiral electric current density increases with the temperature and the chemical potential.

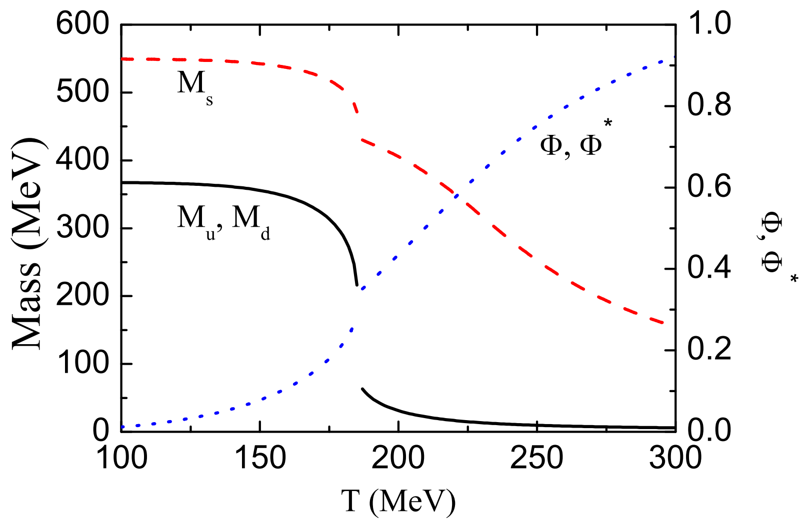

FIG. 2: (color online). Constituent masses of u, d quarks and s quarks, the Polyakov-loop Φ and its conjugate Φ^* as functions of the temperature with $\mu_i = 0$ $(i = u, d, s)$ and $\mu_5 = 250\,\mathrm{MeV}$ $(\mu_5 \equiv \mu_5^u = \mu_5^d = \mu_5^s)$ in the PNJL model with parameters given in the Sec.II.

Next, we turn our attentions to the chiral electric current produced in the three-flavor quark system under an external magnetic field, whose expression is given in Eq. (13). From our above experience that the chiral electric current density would be affected by the particle mass and temperature, we first investigate the dependence of the constituent masses of three-flavor quarks on the temperature during the QCD phase transitions in the PNJL model. Minimizing the thermodynamical potential in Eq. (9) with respect to three-flavor quark condensates, the Polyakov-loop Φ and its conjugate Φ^*, we obtain a set of equations of motion. We neglect the influence of the magnetic field on these equations of motion in our

numerical calculations, since the magnetic field ($eB = 10^2 \sim 10^4\,\mathrm{MeV}^2$ in the non-central heavy-ion collisions [12]) has little impact on these equations of motion. The calculated results are presented in Fig. 2. Here we take the chiral chemical potential $\mu_5 = 250\,\mathrm{MeV}$ for example. In the figure we can find that the constituent masses of u, d quarks and s quarks decrease with the increase of the temperature, and a first order chiral phase transition takes place at the critical temperature $T_C = 185\,\mathrm{MeV}$. The chiral symmetry is restored above this critical temperature and the constituent masses of u, d quarks decrease to their small current masses. Since the s quark has relatively larger current quark mass, its constituent mass is still relatively large when the temperature is larger than T_C, but it is also decreased quickly with the increase of the temperature. In our calculations we also note that when the chiral chemical potential μ_5 is decreased, the value of the critical temperature T_C becomes larger and the first order chiral phase transition gradually evolves to a continuous crossover. Therefore, the influence of the chiral chemical potential μ_5 on the chiral phase transition is similar with that of the quark chemical potential μ. In Fig. 2 we also plot the Polyakov-loop Φ and its conjugate Φ^* versus temperature. One can find that Φ and Φ^* increase from 0 to 1 with the increase of the temperature, implying that the Z(3) symmetry of the gluon field is broken and the deconfinement phase transition takes place [22]. We should emphasize that since the term related with the chiral chemical potential in Eq. (8) does not broken the charge conjugation symmetry, we have $\Phi = \Phi^*$ even μ_5 is nonvanishing, which is different from the quark chemical potential.

In Fig. 3 we show the chiral electric current density of the three-flavor quark system as function of the temperature in the PNJL model. Here we take the external magnetic field $eB = 10^4\,\mathrm{MeV}^2$ for example. First of all, we consider the high temperature limit. In this limit the masses of quarks can be neglected and $\Phi = \Phi^* = 1$. Then the chiral electric current j_3 in Eq. (13) can be easily obtained as

$$j_3 = N_c\Big(\sum_{f=u,d,s} q_f^2\Big)\frac{e^2B\mu_5}{2\pi^2} = \frac{e^2B\mu_5}{\pi^2}. \tag{19}$$

We also plot these high temperature limit values of the chiral electric current density in Fig. 3, i.e. the horizontal lines from bottom to top corresponding to $\mu_5 = 150$, 200, and 250 MeVs, respectively. One can clearly find that when the temperature is high, the system is in the chiral symmetric and deconfined phase, and the chiral electric current density approaches its limit value, i.e. Eq. (19). When the temperature is lowered, especially

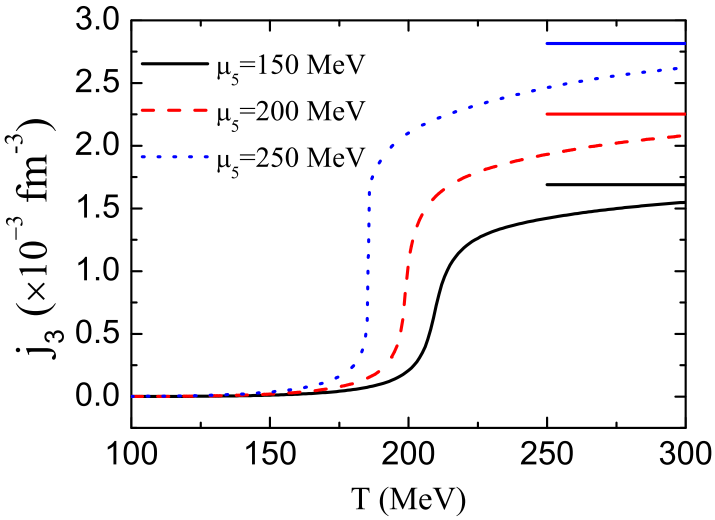

FIG. 3: (color online). Chiral electric current density along the direction of an external magnetic field of the three-flavor quark system j_3 as function of the temperature in the PNJL model with $eB = 10^4\,\mathrm{MeV}^2$, $\mu_i = 0$ ($i = u, d, s$), and several values of the chiral chemical potential μ_5 ($\mu_5 \equiv \mu_5^u = \mu_5^d = \mu_5^s$). The three horizontal lines denote the values of j_3 in the high temperature massless limit, corresponding to $\mu_5 = 150$, 200, and 250 MeVs from bottom to top, respectively.

when the temperature is below the critical temperature T_C, the chiral symmetry is broken and quarks get large constituent masses, then the chiral electric current density along the direction of the external magnetic field is quite suppressed and quickly approaches zero with the decrease of the temperature. This behavior is independent of the value of the chiral chemical potential as Fig. 3 clearly shows. In Fig. 3 we just take magnetic field strength $eB = 10^4\,\mathrm{MeV}^2$ for example, and the chiral electric current density is linearly proportional to the magnetic field strength, since the magnetic field strength B does not enter into the integrations in the expression of j_3, i.e., Eq. (13). Therefore, when the magnetic field strength takes other values, we still have the fact that when the temperature is below the chiral critical temperature T_C, large constituent masses of quarks suppress the chiral electric current drastically.

IV. AZIMUTHAL CHARGED-PARTICLE CORRELATIONS IN HEAVY-ION COLLISIONS

In this section we will try to relate our calculations with experimental observations and investigate how the QCD phase transitions influence on the signals of the chiral magnetic effect. In the experiments of heavy ion collisions, the azimuthal charged-particle correlations, i.e., $\langle \cos(\phi_\alpha + \phi_\beta - 2\Psi_{RP}) \rangle$, are used to detect the $\mathcal{P}$-violating effect [9, 10, 28]. Here ϕ_α and ϕ_β are the azimuthal angles of the produced particles, and α, β represent electric charge $+$ or $-$; Ψ_{RP} is the azimuthal angle of the reaction plane. These angles are depicted in Fig. 4 and in this figure the reaction plane is the plane of $z = 0$ which is perpendicular to the direction of the magnetic field.

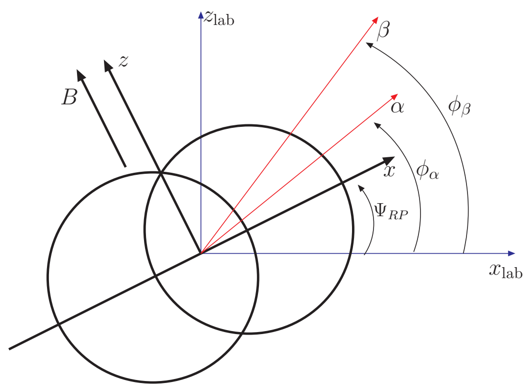

FIG. 4: (color online). Schematic depiction of the transverse plane of a non-central heavy ion collision along the beam-axis (y-axis) (see also Ref. [9]). The plane of $z = 0$ is the reaction plane.

In order to calculate the azimuthal charged-particle correlations, we follow the method of Ref. [12] to define the quantity Δ_+ (Δ_-) which is the positive (negative) electric charge difference in unit of e ($-e$) between on each side of the reaction plane, i.e., the $z = 0$ plane in our notations.

In Fig. 5 we give an schematic illustration of the chiral magnetic effect, and detailed discussions are presented in the caption. From this figure, one can clearly find that it the $\mathcal{P}$-violating effect, i.e., the nonvanishing chiral chemical potential μ_5, that results in the difference of the numbers of the right-handed quarks (anti-quarks) and left-handed quarks (anti-quarks). Then, under an external magnetic field the number of quarks moving along the direction of the magnetic field (i.e., the number of the right-hand quarks in Fig. 5) is

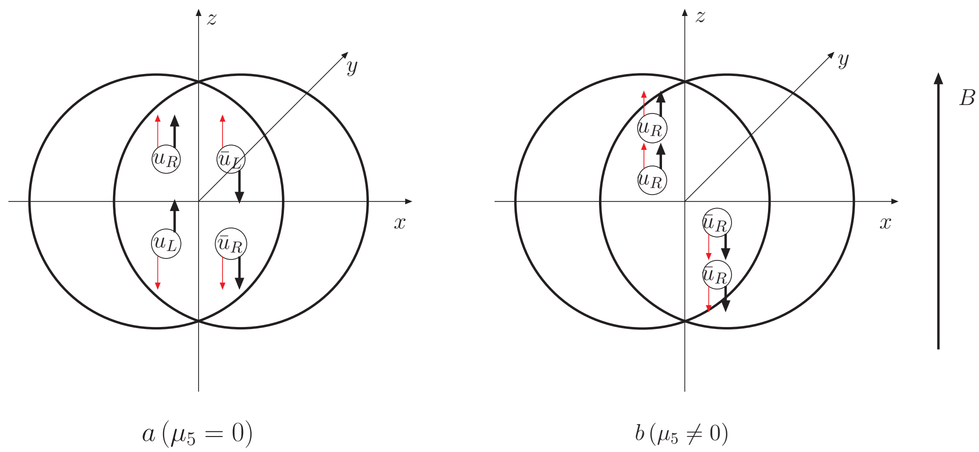

FIG. 5: (color online). Schematic illustrations of the electric charge separation and the chiral magnetic effect (see also Ref. [12]). Here we take "up" quark u and its anti-quark $\bar{u}$ for example. The thick black arrows denote the directions of quark spins and the thin red arrows denote those of the momentum of quarks. a. Under the external magnetic field, quarks in the lowest Landau level (not including quarks in high order Landau levels) are polarized. The spins of u quarks are parallel to the direction of the magnetic field and those of $\bar{u}$ anti-parallel to that direction. In the case of $\mu_5 = 0$, i.e. these is no $\mathcal{P}$-violating effect, the number of right-handed quarks is equal to that of left-handed quarks and so the number of quarks above the $z = 0$ plane is also equal to that of quarks below the $z = 0$ plane. Therefore, when $\mu_5 = 0$ there is no electric charge separation and chiral magnetic effect. b. In the case of $\mu_5 \neq 0$, the number of right-handed quarks is unequal to that of left-handed quarks and the numbers of quarks on two sides of the $z = 0$ plane are different, resulting in the difference of the electric charges between on each side of the reaction plane, which is the electric charge separation effect.

different from that of quarks moving against it (i.e., the number of the left-hand quarks in Fig. 5), and in this way the phenomenon of the electric charge separation takes place as the Fig. 5 b shows.

Considering the simple system composed of only one type of fermion (with positive charge qe) and anti-fermion once more. From the Fig. 5 and the discussions above, we can easily find that the difference of the numbers of positive fermions on each side of the reaction plane is just the difference of the numbers of the right-handed fermions and the left-handed

fermions in the lowest Landau level, which is just

$$
\begin{aligned}
N_5|_{n=0}^{+} &= \Big(\int d^3x\bar{\psi}_R\gamma^0\psi_R - \int d^3x\bar{\psi}_L\gamma^0\psi_L\Big)\Big|_{n=0}^{+} \\
&= \Big(\int d^3x\bar{\psi}\gamma^0\gamma^5\psi\Big)\Big|_{n=0}^{+},
\end{aligned} \tag{20}
$$

where

$$
\psi_R = \frac{1+\gamma^5}{2}\psi \quad \text{and} \quad \psi_L = \frac{1-\gamma^5}{2}\psi. \tag{21}
$$

We should emphasize that the subscript $n = 0$ in Eq. (20) indicates that the difference of the fermion numbers on the two sides of the reaction plane only comes from fermions in the lowest Landau level, since only fermions in the lowest Landau level are polarized, which is proved in Appendix A and Appendix B. The superscript $+$ in Eq. (20) means that only the positive fermions (not the negative anti-fermions) are included. Therefore, employing Eq. (A46) in Appendix A we can further express $N_5|_{n=0}^{+}$ as

$$
\begin{aligned}
N_5|_{n=0}^{+} &= \Big(\int d^3x\bar{\psi}\gamma^0\gamma^5\psi\Big)\Big|_{n=0}^{+} \\
&= V\frac{|q|eB}{2\pi}\sum_{s=\pm1}\int\frac{dp_3}{2\pi}\Big(\frac{s|\epsilon|}{E}\langle a_\epsilon^{s+}a_\epsilon^{s}\rangle\Big)\Big|_{n=0} \\
&= V\frac{|q|eB}{4\pi^2}\Big[\int_0^\infty dp_3\frac{p_3}{E}\frac{1}{e^{(E-\mu-\frac{p_3}{E}\mu_5)/T}+1} - \int_0^\infty dp_3\frac{p_3}{E}\frac{1}{e^{(E-\mu+\frac{p_3}{E}\mu_5)/T}+1}\Big],
\end{aligned} \tag{22}
$$

where E is given by Eq. (17). In the same way, we can obtain the difference of the numbers of negative anti-fermions on each side of the reaction plane, i.e.,

$$
\begin{aligned}
N_5|_{n=0}^{-} &= -\Big(\int d^3x\bar{\psi}\gamma^0\gamma^5\psi\Big)\Big|_{n=0}^{-} \\
&= -V\frac{|q|eB}{2\pi}\sum_{s=\pm1}\int\frac{dp_3}{2\pi}\Big(\frac{s|\epsilon|}{E}\langle b_\epsilon^{s+}b_\epsilon^{s}\rangle\Big)\Big|_{n=0} \\
&= -V\frac{|q|eB}{4\pi^2}\Big[\int_0^\infty dp_3\frac{p_3}{E}\frac{1}{e^{(E+\mu-\frac{p_3}{E}\mu_5)/T}+1} - \int_0^\infty dp_3\frac{p_3}{E}\frac{1}{e^{(E+\mu+\frac{p_3}{E}\mu_5)/T}+1}\Big].
\end{aligned} \tag{23}
$$

Until now, we have obtained the difference of numbers of the positive fermions (negative anti-fermions) between on each side of the reaction plane, so the electric charge difference can be easily obtained as $\Delta_+ = |q|N_5|_{n=0}^{+}$ and $\Delta_- = |q|N_5|_{n=0}^{-}$. We should emphasize that though the electric charge differences Δ_+ and Δ_- are the differences of quark electric charges in our picture, these electric charge differences are conserved through the hadronization processes (or other processes) and are observed in the heavy ion collision experiments,

because the hadronization processes (or other processes) are difficult to result in electric charge separations (for more discussions see Ref. [9, 10]).

The calculations above can be easily extended to the 2+1 flavor quark system, and for this system we have

$$\begin{aligned}
\Delta_+ &= VN_c\frac{eB}{4\pi^2}\Big\{q_u^2\int_0^\infty dp_3\frac{p_3}{E_u}\Big[f\big(E_u-\mu_u-\frac{p_3}{E_u}\mu_5^u\big)-f\big(E_u-\mu_u+\frac{p_3}{E_u}\mu_5^u\big)\Big]\\
&+q_d^2\int_0^\infty dp_3\frac{p_3}{E_d}\Big[\bar{f}\big(E_d+\mu_d-\frac{p_3}{E_d}\mu_5^d\big)-\bar{f}\big(E_d+\mu_d+\frac{p_3}{E_d}\mu_5^d\big)\Big]\\
&+q_s^2\int_0^\infty dp_3\frac{p_3}{E_s}\Big[\bar{f}\big(E_s+\mu_s-\frac{p_3}{E_s}\mu_5^s\big)-\bar{f}\big(E_s+\mu_s+\frac{p_3}{E_s}\mu_5^s\big)\Big]\Big\},
\end{aligned} \tag{24}$$

and

$$\begin{aligned}
\Delta_- &= -VN_c\frac{eB}{4\pi^2}\Big\{q_u^2\int_0^\infty dp_3\frac{p_3}{E_u}\Big[\bar{f}\big(E_u+\mu_u-\frac{p_3}{E_u}\mu_5^u\big)-\bar{f}\big(E_u+\mu_u+\frac{p_3}{E_u}\mu_5^u\big)\Big]\\
&+q_d^2\int_0^\infty dp_3\frac{p_3}{E_d}\Big[f\big(E_d-\mu_d-\frac{p_3}{E_d}\mu_5^d\big)-f\big(E_d-\mu_d+\frac{p_3}{E_d}\mu_5^d\big)\Big]\\
&+q_s^2\int_0^\infty dp_3\frac{p_3}{E_s}\Big[f\big(E_s-\mu_s-\frac{p_3}{E_s}\mu_5^s\big)-f\big(E_s-\mu_s+\frac{p_3}{E_s}\mu_5^s\big)\Big]\Big\},
\end{aligned} \tag{25}$$

where E_f is given by Eq. (11) with $n=0$, and the distribution functions $f(x)$ and $\bar{f}(x)$ for quarks and anti-quarks respectively, are given by Eqs. (14) (15). One could find that when the quark chemical potentials are vanishing, i.e., $\mu_i=0$ ($i=u,d,s$), we have $\Delta_+=-\Delta_-$. In the high temperature limit, the masses of quarks can be neglected and when the quark chemical potentials are vanishing, Eq. (24) and Eq. (25) can be calculated analytically. The results are

$$\Delta_+=-\Delta_-=VN_c\Big(\sum_{f=u,d,s}q_f^2\Big)\frac{eB\mu_5}{4\pi^2}=V\frac{eB\mu_5}{2\pi^2}. \tag{26}$$

In Fig. 6 we show Δ_+/V, where V is the volume of the system, as function of the temperature in the PNJL model with $eB=10^4\,\mathrm{MeV}^2$, $\mu_i=0$, and several values of the chiral chemical potential μ_5. In fact, the dependence of Δ_+/V on the temperature is similar with that of the chiral electric current density. When the temperature is above the critical temperature of the chiral phase transition, Δ_+/V approaches its high temperature limit value given in Eq. (26), which is shown in Fig. 6 by the horizontal lines. However, once the temperature is decreased to that below the critical temperature, chiral symmetry is broken and quarks get large constituent masses, which results in that the electric charge difference between on each side of the reaction plane is suppressed drastically.

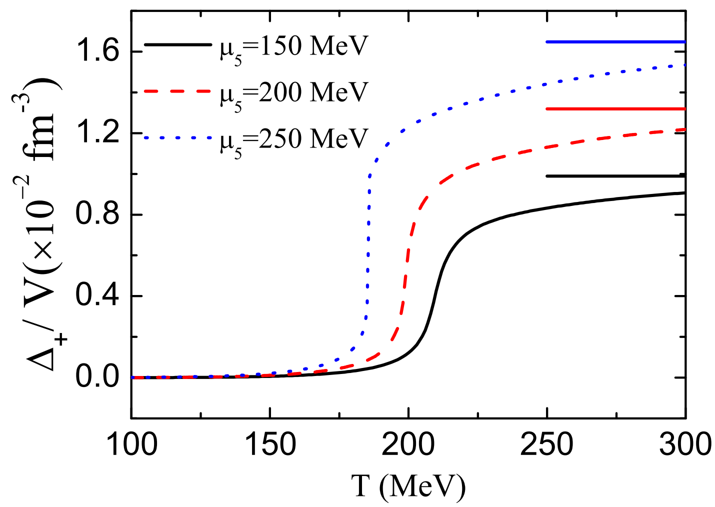

FIG. 6: (color online). Ratio of the positive electric charge difference between on each side of the reaction plane and the volume of the system, i.e., Δ_+/V, as function of the temperature in the PNJL model with $eB = 10^4\,\mathrm{MeV}^2$, $\mu_i = 0$ $(i = u, d, s)$, and several values of the chiral chemical potential μ_5. The three horizontal lines denote the values of Δ_+/V in the high temperature massless limit, corresponding to $\mu_5 = 150$, 200, and 250 MeVs from bottom to top, respectively.

In order to determine the azimuthal charged-particle correlations in heavy ion collisions, we need to calculate the quantity N_+ (N_-) which is the total positive (negative) electric charge number in unit of e $(-e)$ on both sides of the reaction plane. Considering the simple system composed of only one type of fermion (with positive charge qe) and anti-fermion, we can easily find that the total positive (negative) electric charge is the sum of the positive (negative) electric charge of the right-handed and left-handed fermions (anti-fermions), i.e.

$$\begin{aligned} N_+ &= |q|\Big(\int d^3x\bar{\psi}_R\gamma^0\psi_R + \int d^3x\bar{\psi}_L\gamma^0\psi_L\Big)\Big|^+ \\ &= |q|\Big(\int d^3x\bar{\psi}\gamma^0\psi\Big)\Big|^+ \\ &= V|q|^2\frac{eB}{2\pi}\sum_{n=0}^{\infty}\sum_{s=\pm1}\int\frac{dp_3}{2\pi}\Big(\langle a_\epsilon^{s+}a_\epsilon^s\rangle\Big) \\ &= V|q|^2\frac{eB}{2\pi}\sum_{n=0}^{\infty}\Big[\int\frac{dp_3}{2\pi}\frac{1}{e^{(E-\mu-\frac{|\epsilon|}{E}\mu_5)/T}+1} + \int\frac{dp_3}{2\pi}\frac{1}{e^{(E-\mu+\frac{|\epsilon|}{E}\mu_5)/T}+1}\Big], \end{aligned} \tag{27}$$

where we have

$$|\epsilon| = \sqrt{2n|q|eB + p_3^2} \tag{28}$$

and

$$E=\sqrt{2n|q|eB+p_3^2+m^2}. \tag{29}$$

The superscript + on the right hand of the vertical line in Eq. (27) denotes that only fermions with positive charge are included (not including negative anti-fermions). We should emphasize that all Landau levels are summed in Eq. (27), which is different from the electric charge difference between on each side of the reaction plane in Eq. (22), where only particles in the lowest Landau level contribute to the charge asymmetry. In the same way, one can also obtain

$$\begin{aligned}
N_- &= -|q|\Big(\int d^3x\bar{\psi}\gamma^0\psi\Big)\Big|^- \\
&= V|q|^2\frac{eB}{2\pi}\sum_{n=0}^{\infty}\sum_{s=\pm1}\int\frac{dp_3}{2\pi}\Big(\langle b_\epsilon^{s+}b_\epsilon^s\rangle\Big) \\
&= V|q|^2\frac{eB}{2\pi}\sum_{n=0}^{\infty}\Big[\int\frac{dp_3}{2\pi}\frac{1}{e^{(E+\mu-\frac{|\epsilon|}{E}\mu_5)/T}+1}+\int\frac{dp_3}{2\pi}\frac{1}{e^{(E+\mu+\frac{|\epsilon|}{E}\mu_5)/T}+1}\Big],
\end{aligned} \tag{30}$$

Similarly, for the 2+1 flavor quark system we can obtain

$$\begin{aligned}
N_+ = VN_c\frac{eB}{2\pi}\sum_{n=0}^{\infty}\sum_{s=\pm1}&\Big[q_u^2\int\frac{dp_3}{2\pi}f\big(E_u-\mu_u-\frac{s|\epsilon_u|}{E_u}\mu_5^u\big) \\
&+q_d^2\int\frac{dp_3}{2\pi}\bar{f}\big(E_d+\mu_d-\frac{s|\epsilon_d|}{E_d}\mu_5^d\big) \\
&+q_s^2\int\frac{dp_3}{2\pi}\bar{f}\big(E_s+\mu_s-\frac{s|\epsilon_s|}{E_s}\mu_5^s\big)\Big].
\end{aligned} \tag{31}$$

and

$$\begin{aligned}
N_- = VN_c\frac{eB}{2\pi}\sum_{n=0}^{\infty}\sum_{s=\pm1}&\Big[q_u^2\int\frac{dp_3}{2\pi}\bar{f}\big(E_u+\mu_u-\frac{s|\epsilon_u|}{E_u}\mu_5^u\big) \\
&+q_d^2\int\frac{dp_3}{2\pi}f\big(E_d-\mu_d-\frac{s|\epsilon_d|}{E_d}\mu_5^d\big) \\
&+q_s^2\int\frac{dp_3}{2\pi}f\big(E_s-\mu_s-\frac{s|\epsilon_s|}{E_s}\mu_5^s\big)\Big].
\end{aligned} \tag{32}$$

We should comment that in Eqs. (31) (32) we have assumed that the total positive (negative) electric charges of the quarks and anti-quarks in the fireball at early stage are conserved through the subsequent evolution of the QGP and are observed by the multiplicities of the produced charged particles in experiments. Although this is an assumption, it is reasonable. Because if the centrality is fixed and the collision energy is increased, on the one hand, the

temperature of the QGP at early stage is increased, which results in that the total positive or negative electric charges of quarks and anti-quarks increase, on the other hand, the increase of the collision energy will lead to the increase of the multiplicities of the produced charged particles. Therefore, the total positive (negative) electric charges of the charged particles produced in heavy ion collisions increase with those of the quarks and anti-quarks.

So far, we can calculate the azimuthal charged particle correlations $\langle\cos(\phi_\alpha+\phi_\beta-2\Psi_{RP})\rangle$ in heavy ion collisions. With the notation $a_{\alpha\beta}\equiv-\langle\cos(\phi_\alpha+\phi_\beta-2\Psi_{RP})\rangle$, it can be shown that [12]

$$a_{++}=\frac{\pi^2}{16}\frac{\langle\Delta_+^2\rangle}{N_+^2},\quad a_{--}=\frac{\pi^2}{16}\frac{\langle\Delta_-^2\rangle}{N_-^2},\tag{33}$$

and

$$a_{+-}=\frac{\pi^2}{16}\frac{\langle\Delta_+\Delta_-\rangle}{N_+N_-},\tag{34}$$

where the azimuthal angle distribution of the charged particles is assumed to be

$$\frac{dN_\pm}{d\phi}=\frac{1}{2\pi}N_\pm+\frac{1}{4}\Delta_\pm\sin(\phi-\Psi_{RP}).\tag{35}$$

Since we mainly focus on the influence of the QCD phase transitions, especially the chiral phase transition, on the chiral magnetic effect in this work, we will neglect the screening suppression effect due to the final state interactions [12] and make $\mu_i=0$ $(i=u,d,s)$, then we have $a_{++}=a_{--}=-a_{+-}$. Therefore, we only study a_{++} in the following.

In Fig. 7 we show a_{++} defined in Eq. (33) as function of the temperature at several values of the chiral chemical potential μ_5 ($\mu_5\equiv\mu_5^u=\mu_5^d=\mu_5^s$) and the magnetic field strength. We find that there is a pronounced cusp in a_{++} at the critical temperature during the chiral phase transition (the critical temperature $T_c=209\,\mathrm{MeV}$ for $\mu_5=150\,\mathrm{MeV}$ and $T_c=185\,\mathrm{MeV}$ for $\mu_5=250\,\mathrm{MeV}$ in the PNJL model). From the Fig. 7 one can also find that although the value of a_{++} is proportional to the square of the magnetic field strength, the shape of the curve for a_{++} as function of temperature is almost independent of the magnetic field strength. Furthermore, the cusp at the critical temperature in the curve becomes much sharper with the increase of the chiral chemical potential. With the decrease of the temperature, when the temperature is below T_c, chiral symmetry is dynamically broken and quarks obtain large constituent masses. We should emphasize that it is the large quark mass that results in the drastic suppression of the chiral electric current density (see Sec. III), the electric charge difference between on each side of the reaction plane (see Fig. 6),

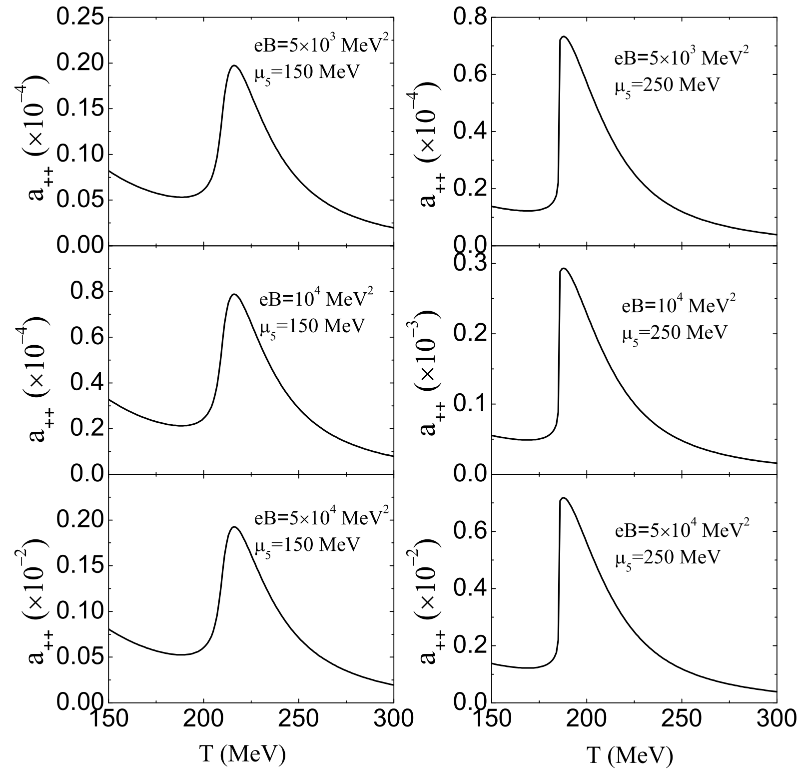

FIG. 7: Correlation a_{++} as function of the temperature calculated in the PNJL model with $\mu_5 = 150\,\mathrm{MeV}$ (left panel) and $\mu_5 = 250\,\mathrm{MeV}$ (right panel). The magnetic field corresponds to $eB = 5 \times 10^3$, 10^4, and $5 \times 10^4\,\mathrm{MeV}^2$ from top to bottom, respectively.

and the azimuthal charged particle correlations. Furthermore, the chiral magnetic effect is close related with the axial anomaly [12]. Without axial anomaly there would not be the chiral magnetic effect. Since the axial anomaly can be suppressed by the mass effect, which has been discussed in detail in Ref. [29], it is natural to expect that the chiral magnetic effect can also be suppressed by large constituent quark masses. Therefore, it is reasonable that the azimuthal charged particle correlations described by a_{++} (a_{--} and a_{+-}) defined in Eqs. (33) (34) are quite decreased once the temperature is below the critical temperature. It can been seen from Fig. 7 that, when the temperature is above T_c, a_{++} decreases with the increase of the temperature, which is because higher temperature makes it more difficult to polarize quarks with magnetic field and thus suppresses the charge separation effect.

What do our calculated results imply in future energy scanning experiments of heavy ion collisions? With the decrease of the heavy ion collision energy, the temperature of the QGP

produced in the fireball at early stage is also decreased. Since the magnetic field produced in non-central collisions decays with time [12], the observed charge separation mainly carries the information of the QGP at early stage. Therefore, we expect that when the collision energy is decreased to a value that cannot drive the chiral phase transition, the azimuthal charged particle correlations (especially for the same charge correlations, because the opposite charge correlations are suppressed by final state interactions) are quite suppressed. So this property can be employed to search for where the QCD phase transitions take place.

From the calculations of the azimuthal charged particle correlations $\langle\cos(\phi_\alpha+\phi_\beta-2\Psi_{RP})\rangle$ above, we can find that there are some uncertainties on the total positive (negative) electric charges of the produced charged particles N_+ (N_-). This little defect motivate us to search for other better correlators which are not divided by the square of N_+ or N_-. In fact, this kind of correlators has been proposed by D.E.Kharzeev and his collaborators [12]. In the following we compare these two kinds of correlators briefly. First of all, we make $(\phi_\alpha - \Psi_{RP}) \to \phi_\alpha$ and $(\phi_\beta - \Psi_{RP}) \to \phi_\beta$, and then the ϕ_α and ϕ_β are the azimuthal angles of produced particles with respective to the reaction plane as Fig. 4 shows. For each collision event, we follow the definition of the correlators in Ref. [12], i.e.,

$$f(\phi_\alpha,\phi_\beta) = \frac{1}{N_\alpha N_\beta}\sum_{i=1}^{N_\alpha}\sum_{j=1}^{N_\beta}\cos(\phi_{\alpha i}+\phi_{\beta j}). \tag{36}$$

In the same way, here $\alpha,\beta=\pm$ denotes the electric charge. In order to remove the multiplicity fluctuations the correlators are averaged over N_e similar events. Then one obtain

$$\begin{aligned} a_{\alpha\beta} &= -\langle\cos(\phi_\alpha+\phi_\beta)\rangle \\ &= -\frac{1}{N_e}\sum_{n=1}^{N_e} f(\phi_\alpha,\phi_\beta), \end{aligned} \tag{37}$$

where the correlators $a_{\alpha\beta}$ are those calculated in Fig. 7. Furthermore, correlators which are not divided by square of the total multiplicity of charged particles are also proposed by D.E.Kharzeev and his collaborators and are thought to be very useful, which are

$$b_{\alpha\beta} = -\frac{1}{N_e}\sum_{n=1}^{N_e} g(\phi_\alpha,\phi_\beta), \tag{38}$$

with

$$g(\phi_\alpha,\phi_\beta) = \sum_{i=1}^{N_\alpha}\sum_{j=1}^{N_\beta}\cos(\phi_{\alpha i}+\phi_{\beta j}). \tag{39}$$

Same as the $a_{\alpha\beta}$, it can be found that

$$b_{++} = \frac{\pi^2}{16}\langle \Delta_+^2 \rangle, \quad b_{--} = \frac{\pi^2}{16}\langle \Delta_-^2 \rangle, \tag{40}$$

and

$$b_{+-} = \frac{\pi^2}{16}\langle \Delta_+ \Delta_- \rangle. \tag{41}$$

In Fig. 6 we have calculated the Δ_+/V as function of the temperature during the QCD phase transitions, and find that Δ_+/V is rapidly suppressed and approaches zero when the temperature is below the chiral critical temperature. Within similar collision events (similar centrality and atomic number), it can be expected that the dependence of the volume of the fireball at the early stage on the collision energy is mild. Therefore, it can be predicted that with the decrease of the collision energy, the correlators $b_{\alpha\beta}$, which are the azimuthal charged particle correlations not divided by the square of the total multiplicity of charged particles, get a sudden suppression at the critical temperature of the QCD phase transitions and approaches zero rapidly.

V. SUMMARY AND DISCUSSIONS

In this work, we have studied the influence of the QCD phase transitions on the chiral magnetic effect. The chiral electric current density, the electric charge difference between on each side of the reaction plane, and the azimuthal charged particle correlations in heavy ion collisions are calculated in the PNJL model, and their dependence on the temperature are studied. We find that with the decrease of the temperature, the chiral electric current density and the electric charge difference between on each side of the reaction plane are suppressed abruptly at the critical temperature of the QCD phase transitions and approach zero rapidly, since below the critical temperature the chiral symmetry is broken and quarks obtain large constituent mass. It is the large quark mass that suppresses not only the axial anomaly but also the chiral magnetic effect. For the azimuthal charged particle correlations, we study not only the correlators $a_{\alpha\beta}$, which are the correlators divided by the square of the total multiplicity of charged particles and are measured in current experiments, but also another kind of correlators $b_{\alpha\beta}$ which are not divided by the square of the total multiplicity. We find that both $a_{\alpha\beta}$ and $b_{\alpha\beta}$ get a sudden suppression at the critical temperature of the QCD phase transitions. Furthermore, the correlators $b_{\alpha\beta}$ approaches zero rapidly once

the temperature decreases to values that are below the critical temperature. Therefore, It indicates that azimuthal charged particle correlations (both $a_{\alpha\beta}$ and $b_{\alpha\beta}$, in fact $b_{\alpha\beta}$ is better because the correlators $b_{\alpha\beta}$ remove the fluctuations of the total multiplicity of charged particles) can be used as a signal to identify the chiral phase transition in the energy scan experiment in RHIC.

We should discuss the possibility that using the azimuthal charged particle correlations ($a_{\alpha\beta}$ and $b_{\alpha\beta}$) to search for where the QCD phase transitions take place in future energy scanning experiments in RHIC. In order to simplify the calculations, we make the magnetic field strength and the chiral chemical potential fixed across the QCD phase transitions in this work. In the realistic situations the magnetic field decays with time and the chiral chemical potential has some distribution. However, we think that our simplification is reasonable and would not change our conclusions. The reasons are listed below:

(1) In this work we are concentrated on the influence of the QCD phase transitions, especially the chiral phase transition, on the chiral magnetic effect embodied by the phenomenon of the charge separation. Since the chiral phase transition takes place during a very narrow region of the temperature (or the collision energy equivalently) as Fig. 2 shows, the dependence of the magnetic field and the chiral chemical potential on the temperature is limited in this narrow region.

(2) Indeed the magnetic field decays with time in a collision event, which has been confirmed in Ref. [12]. However, what influences on our calculations is the dependence of the magnetic field in the fireball at early stage on the collision energy (different events with different collision energy). Why is the magnetic field at the early stage of the evolution of the fireball? This is because the electric charge difference between on each side of the reaction plane $\Delta_{\pm}$ (describing the magnitude of the charge separation) is proportional to the magnetic field strength as Eqs. (24) (25) show (we should emphasize that the total multiplicity of the charged particle $N_{\pm}$ is almost not affected by the magnetic field with value $eB = 10^2 \sim 10^4\,\mathrm{MeV}^2$ in the non-central heavy ion collisions). Therefore, the electric charge difference coming from the early stage of the fireball evolution is much larger than that from the late stage, since the magnetic field at early stage is larger than that at late stage. So we are more concerned about the magnetic field at early stage. Fortunately, for similar collision events (similar centrality and atomic

number), the dependence of the magnetic field on the collision energy is very mild (comparing Fig.A.1. (center of mass energy per nucleon pair being $\sqrt{s} = 62\,\text{GeV}$) with Fig.A.2 ($\sqrt{s} = 200\,\text{GeV}$) in Ref. [12]). This is because what determines the magnetic field is the velocity of the heavy ion for similar collision events. However, for $\sqrt{s} = 200\,\text{GeV}$ the velocity of the heavy ion is $v = 0.99995c$ where c is the light speed; for $\sqrt{s} = 62\,\text{GeV}$ the velocity of the heavy ion is $v = 0.99948c$. Therefore, although the difference of the two collision energy is quite large, the difference of their corresponding velocity of the heavy ion is quite small, which results in that the difference of the magnetic field is small.

(3) As for the chiral chemical potential, we should comment that in the chiral symmetry broken phase, quarks get constituent mass. It is found that the mass always causes the asymmetry between the number of right-handed and left-handed fermions to decay [31], i.e., the chiral chemical potential decreases with time in the chiral symmetry broken phase. Our calculations above indicate that when the temperature is decreased and crosses the critical temperature of the chiral phase transition, large quark constituent mass suddenly suppresses the electric charge difference between on each side of the reaction plane. These calculations are performed with the chiral chemical potential fixed. If we further consider that the chiral chemical potential is reduced when the temperature is below the critical temperature, the suppression is much more significant.

(4) In this work we perform our calculations with multi-values for the magnetic field strength and the chiral chemical potential (see Fig. 3, Fig. 6, and Fig. 7). For all these values we find the same conclusion that in the chiral symmetry broken phase, the chiral magnetic effect is quite suppressed and almost vanishes. Therefore, the chiral magnetic effect can be used as an order parameter of the QCD phase transitions.

(5) We should emphasize that the physical essence underlying our calculated results is very important. It is the large mass that suppresses the axial anomaly and the asymmetry between the number of right-handed and left-handed fermions, which is verified in general quantum field theory [29, 31]. When the mass of the fermion approaches infinity, there would be of course no difference between right- and left-handed fermions. Therefore, our calculated results is consistent with this basic principle and verify the

conjecture proposed by D.E.Kharzeev and his collaborators that the chiral magnetic effect can be used as an order parameter for the QCD phase transition [12].

Acknowledgments

This work was supported by the National Natural Science Foundation of China under contract Nos. 10425521, 10675007, 10935001, the Major State Basic Research Development Program under contract Nos. G2007CB815000. One of the authors (W.J.F.) would also acknowledge the financial support from China Postdoctoral Science Foundation No. 20090460534.

Appendix A: Thermodynamics of a fermion system with $\mathcal{P}$ violation and under a background magnetic field

Considering a system composed of only one type of fermion with positive charge e and mass m, and a homogeneous magnetic field with strength B is along the positive z direction. Assuming the system is in thermodynamical equilibrium with temperature T and chemical potential μ. In order to include the effects of $\mathcal{P}$ and $\mathcal{CP}$ violation, we follow the method of Ref. [15] to introduce the chiral chemical potential μ_5. We begin with the partition function of the system as

$$Z = \mathrm{Tr} e^{-\beta(\hat{H}-\mu\hat{N}-\mu_5\hat{N}_5)}, \tag{A1}$$

where $\beta = 1/T$ and quantities with hat are operators, and the Hamiltonian $\hat{H}$ is

$$\hat{H} = \int d^3x\mathcal{H} = \int d^3x\bar{\psi}(-i\gamma^i\partial_i - e\gamma^i A^i + m)\psi, \tag{A2}$$

here $i = 1, 2, 3$. The Hamiltonian density $\mathcal{H}$ above can be obtained from the lagrangian density given by

$$\mathcal{L} = \bar{\psi}(i\gamma^\mu D_\mu - m)\psi, \tag{A3}$$

where $D_\mu = \partial_\mu + ieA_\mu$ and $\mu = 0, 1, 2, 3$. In the Hamiltonian Eq. (A2), we have used the fact that since we only consider the case with homogenous magnetic field along the positive z direction, we can assume $A_1 = -(1/2)Bx_2$ and $A_2 = (1/2)Bx_1$. $\hat{N}$ and $\hat{N}_5$ in the partition

function in Eq. (A1) are

$$\hat{N} = \int d^3x \bar{\psi}\gamma^0\psi, \tag{A4}$$

$$\hat{N}_5 = \int d^3x \bar{\psi}\gamma^0\gamma^5\psi, \tag{A5}$$

respectively.

First of all, we should solve the Dirac equation with a magnetic field, i.e.

$$i\partial_0\psi = \Big[(-i\partial_i - eA^i)\gamma^0\gamma^i + \gamma^0 m\Big]\psi. \tag{A6}$$

In the following, we employ the notations in Ref. [30] and use the chiral representation of the γ matrices, i.e.

$$\gamma^0 = \begin{pmatrix} 0 & 1 \\ 1 & 0 \end{pmatrix}, \quad \gamma^i = \begin{pmatrix} 0 & \sigma^i \\ -\sigma^i & 0 \end{pmatrix}, \quad \gamma^5 = \begin{pmatrix} -1 & 0 \\ 0 & 1 \end{pmatrix}. \tag{A7}$$

We express the four-component spinor as two two-component left-handed and right handed Weyl spinors, i.e.

$$\psi = \begin{pmatrix} \psi_L \\ \psi_R \end{pmatrix}. \tag{A8}$$

Then, for the positive energy solution, the Dirac equation (A6) can be expressed as

$$\begin{pmatrix} -(-i\partial_i - eA^i)\sigma^i & m \\ m & (-i\partial_i - eA^i)\sigma^i \end{pmatrix}\begin{pmatrix} \psi_L \\ \psi_R \end{pmatrix} = E\begin{pmatrix} \psi_L \\ \psi_R \end{pmatrix}. \tag{A9}$$

We set $H_+ \equiv (-i\partial_i - eA^i)\sigma^i$, then if we find an appropriate right handed spinor ψ_R, which is an eigenfunction of the H_+ with eigenvalue ϵ, i.e.

$$H_+\psi_R = \epsilon\psi_R, \tag{A10}$$

we have $E^2 = \epsilon^2 + m^2$ and

$$\psi_L = \frac{(E-\epsilon)}{m}\psi_R. \tag{A11}$$

We set $\psi_R = \sqrt{E+\epsilon}\xi^s$, therefore, we have $\psi_L = \sqrt{E-\epsilon}\xi^s$ and $H_+\xi^s = \epsilon\xi^s$.

For the negative energy solution of the Dirac equation (A6), we have

$$\begin{pmatrix} H_- & m \\ m & -H_- \end{pmatrix}\begin{pmatrix} \psi_L \\ \psi_R \end{pmatrix} = -E\begin{pmatrix} \psi_L \\ \psi_R \end{pmatrix}. \tag{A12}$$

where we set $H_- \equiv -H_+ = (i\partial_i + eA^i)\sigma^i$. In the same way, if we find a $\xi^{-(s)}$ satisfying $H_-\xi^{-(s)} = \epsilon\xi^{-(s)}$, then we can obtain

$$\psi = \begin{pmatrix} \sqrt{E-\epsilon}\,\xi^{-(s)} \\ -\sqrt{E+\epsilon}\,\xi^{-(s)} \end{pmatrix}. \tag{A13}$$

In the following, we will solve the eigenvalue equation

$$H_+\xi^s = \epsilon\xi^s, \tag{A14}$$

and here,

$$\begin{aligned} H_+ &= (-i\partial_i - eA^i)\sigma^i \\ &= -i\partial_3\sigma^3 + (-i\partial_a - eA^a)\sigma^a \\ &= p^3\sigma^3 + H_\perp, \end{aligned} \tag{A15}$$

where $a = 1,2$ and in the last line we have used the fact that A^i is independent of x_3 and $A^3 = 0$, so the eigenstates in the x_3 direction are free continuum of momentum. We should note that since $\{\sigma^3, H_\perp\} = 0$, if there is a eigenstate $|\lambda\rangle$ of $H_\perp$ with eigenvalue $\lambda > 0$, there must be another eigenstate $\sigma^3|\lambda\rangle$ of $H_\perp$ with eigenvalue $-\lambda < 0$. In the representation of $|\lambda\rangle$ and $\sigma^3|\lambda\rangle$, Eq. (A14) can be expressed as

$$\begin{pmatrix} \lambda & p^3 \\ p^3 & -\lambda \end{pmatrix}\begin{pmatrix} c_1 \\ c_2 \end{pmatrix} = \epsilon\begin{pmatrix} c_1 \\ c_2 \end{pmatrix}, \tag{A16}$$

where $\xi^s = (c_1, c_2)^T$. Eq. (A16) has two solutions which are

$$\xi^1 = \frac{1}{\sqrt{2|\epsilon|}}\begin{pmatrix} \mathrm{sgn}(p_3)\sqrt{|\epsilon|+\lambda} \\ \sqrt{|\epsilon|-\lambda} \end{pmatrix}, \quad \text{with} \quad \epsilon = |\epsilon|, \tag{A17}$$

and

$$\xi^{-1} = \frac{1}{\sqrt{2|\epsilon|}}\begin{pmatrix} -\mathrm{sgn}(p_3)\sqrt{|\epsilon|-\lambda} \\ \sqrt{|\epsilon|+\lambda} \end{pmatrix}, \quad \text{with} \quad \epsilon = -|\epsilon|, \tag{A18}$$

where $|\epsilon| = \sqrt{\lambda^2 + p_3^2}$ and ξ^s has been normalized. Here we have use p_3 to stand for p^3 without confusion. Equations (A17) (A18) can also be unified to express as

$$\xi^s = \frac{1}{\sqrt{2|\epsilon|}}\begin{pmatrix} (s)\mathrm{sgn}(p_3)\sqrt{|\epsilon|+s\lambda} \\ \sqrt{|\epsilon|-s\lambda} \end{pmatrix}, \quad \text{with} \quad \epsilon = s|\epsilon|. \tag{A19}$$

In the same way, we can solve $H_-\xi^{-(s)} = \epsilon\xi^{-(s)}$ for the anti-particle, i.e.,

$$\xi^{-(s)} = \frac{1}{\sqrt{2|\epsilon|}}\begin{pmatrix} (-s)\mathrm{sgn}(p_3)\sqrt{|\epsilon| - s\lambda} \\ \sqrt{|\epsilon| + s\lambda} \end{pmatrix}, \quad \text{with} \quad \epsilon = -s|\epsilon|. \tag{A20}$$

Next, we turn to the eigen-equation of the transverse momentum $H_\perp|\lambda\rangle = \lambda|\lambda\rangle$. It is obvious that we also have

$$H_\perp^2|\lambda\rangle = \lambda^2|\lambda\rangle. \tag{A21}$$

$H_\perp^2$ can be directly calculated as

$$\begin{aligned} H_\perp^2 &= [(-i\partial_a - eA^a)\sigma^a]^2 \\ &= \big(-i\frac{\partial}{\partial x_1}\big)^2 + \big(-i\frac{\partial}{\partial x_2}\big)^2 + \frac{1}{4}e^2B^2(x_1^2 + x_2^2) \\ &\quad -eB\big[x_1\big(-i\frac{\partial}{\partial x_2}\big) - x_2\big(-i\frac{\partial}{\partial x_1}\big)\big] - eB\sigma^3. \end{aligned} \tag{A22}$$

The physical meanings of Eq. (A22) are very clear. The second line of Eq. (A22) indicates that the dynamics of particles in the transverse plane, which is perpendicular to the magnetic field, is the two dimensional homogeneous harmonic oscillation. The last line of Eq. (A22) includes contributions from the orbital and spin angular momentum in the z direction. Rescaling $x_1 \to (eB/2)^{1/2}x_1$, $x_2 \to (eB/2)^{1/2}x_2$, and$H_\perp^2 \to H_\perp^2/eB$, we find

$$H_\perp^2 = \frac{1}{2}[(p_1^2 + x_1^2) + (p_2^2 + x_2^2)] - (l_3 + \sigma^3), \tag{A23}$$

where $p_a = -i\partial/\partial x_i$ $(i = 1, 2)$ and $l_3 = x_1p_2 - x_2p_1$. In the following, we use the algebraic method to solve the problem of eigenvalue. Introducing annihilation and creation operators

$$\begin{aligned} a_i &= \frac{1}{\sqrt{2}}(x_i + ip_i), \\ a_i^+ &= \frac{1}{\sqrt{2}}(x_i - ip_i). \end{aligned} \tag{A24}$$

It can be easily verified that

$$[a_i, a_j] = 0 \quad \text{and} \quad [a_i, a_j^+] = \delta_{ij}, \tag{A25}$$

thus these operators are annihilation and creation operators of boson. Employing these operators we obtain

$$H_\perp^2 = a_1^+a_1 + a_2^+a_2 + 1 - (l_3 + \sigma^3), \tag{A26}$$

with

$$l_3 = i(-a_1^+ a_2 + a_2^+ a_1). \tag{A27}$$

To diagonalize the orbital angular momentum l_3, we introduce two another pairs of annihilation and creation operators, and the annihilation operators are

$$\begin{aligned} a_+ &= \frac{1}{\sqrt{2}}(a_1 - ia_2), \\ a_- &= \frac{1}{\sqrt{2}}(a_1 + ia_2). \end{aligned} \tag{A28}$$

In the same way, it can be verified that they are also bosonic operators. Consequently, we can obtain

$$l_3 = a_+^+ a_+ - a_-^+ a_-, \tag{A29}$$

and

$$a_1^+ a_1 + a_2^+ a_2 = a_+^+ a_+ + a_-^+ a_-. \tag{A30}$$

Therefore, we finally have

$$H_\perp^2 = 2a_-^+ a_- + 1 - \sigma^3 = \begin{pmatrix} 2a_-^+ a_- & 0 \\ 0 & 2(a_-^+ a_- + 1) \end{pmatrix}. \tag{A31}$$

Here $a_-^+ a_-$ is the boson number operators, and its eigenvalue can be denoted as n (n=0,1,2...). Recovering eB we obtain the eigenvalue of Eq. (A21) with $\lambda^2 = 2neB$. We should emphasize that from Eq. (A31) one can find that states of $n > 0$ are degenerate with two different spins, while for $n = 0$ state, there is only one spin. Therefore, this means that only particles in the lowest level are polarized by the external magnetic field.

Until now, we have solved the Dirac equation under a background magnetic field. We summarize the results here. The wave function of the fermion is given as

$$u^s = \begin{pmatrix} \sqrt{E - \epsilon}\xi^s \\ \sqrt{E + \epsilon}\xi^s \end{pmatrix}, \quad \text{with} \quad s = \pm 1. \tag{A32}$$

When $n > 0$,

$$\xi^s = \frac{1}{\sqrt{2|\epsilon|}} \begin{pmatrix} (s)\mathrm{sgn}(p_3)\sqrt{|\epsilon| + s\lambda} \\ \sqrt{|\epsilon| - s\lambda} \end{pmatrix}, \quad \text{with} \quad \epsilon = s|\epsilon|; \tag{A33}$$

when $n = 0$,

$$\xi^1 = \begin{cases} (1,0)^T & \text{for} \quad p_3 > 0 \\ (0,1)^T & \text{for} \quad p_3 < 0 \end{cases}, \quad \text{with} \quad \epsilon = |p_3|, \tag{A34}$$

$$\xi^{-1} = \begin{cases} (0,1)^T & \text{for} \quad p_3 > 0 \\ (1,0)^T & \text{for} \quad p_3 < 0 \end{cases}, \quad \text{with} \quad \epsilon = -|p_3|. \tag{A35}$$

The wave function of the anti-fermion is

$$v^s = \begin{pmatrix} \sqrt{E-\epsilon}\,\xi^{-(s)} \\ -\sqrt{E+\epsilon}\,\xi^{-(s)} \end{pmatrix}, \quad \text{with} \quad s = \pm 1. \tag{A36}$$

When $n > 0$,

$$\xi^{-(s)} = \frac{1}{\sqrt{2|\epsilon|}} \begin{pmatrix} (-s)\mathrm{sgn}(p_3)\sqrt{|\epsilon| - s\lambda} \\ \sqrt{|\epsilon| + s\lambda} \end{pmatrix}, \quad \text{with} \quad \epsilon = -s|\epsilon|; \tag{A37}$$

when $n = 0$,

$$\xi^{-(1)} = \begin{cases} (0,1)^T & \text{for} \quad p_3 > 0 \\ (1,0)^T & \text{for} \quad p_3 < 0 \end{cases}, \quad \text{with} \quad \epsilon = -|p_3|, \tag{A38}$$

$$\xi^{-(-1)} = \begin{cases} (1,0)^T & \text{for} \quad p_3 > 0 \\ (0,1)^T & \text{for} \quad p_3 < 0 \end{cases}, \quad \text{with} \quad \epsilon = |p_3|. \tag{A39}$$

In the equations above, we have

$$\lambda = \sqrt{2neB}, \tag{A40}$$

$$|\epsilon| = \sqrt{\lambda^2 + p_3^2} = \sqrt{2neB + p_3^2}, \tag{A41}$$

$$E = \sqrt{|\epsilon|^2 + m^2} = \sqrt{2neB + p_3^2 + m^2}. \tag{A42}$$

It should be emphasized that $s = +1$ represents the state that the spin of a fermion or anti-fermion parallels to its momentum, i.e. the right-handed state, while $s = -1$ corresponds to the state that the spin anti-parallels to the momentum and thus is the left-handed state. Therefore, the helicity of a fermion is s and that of a anti-fermion is $-s$.

Employing the standard canonical quantization procedure, we can express the Hamiltonian H in Eq. (A2) as

$$\begin{aligned} \hat{H} &= V\frac{eB}{2\pi}\sum_{n=0}^{\infty}\sum_{s=\pm1}\int\frac{dp_3}{2\pi}E(a_\epsilon^{s+}a_\epsilon^s - b_\epsilon^s b_\epsilon^{s+}) \\ &= V\frac{eB}{2\pi}\sum_{n=0}^{\infty}\sum_{s=\pm1}\int\frac{dp_3}{2\pi}E(a_\epsilon^{s+}a_\epsilon^s + b_\epsilon^{s+}b_\epsilon^s - 1), \end{aligned} \tag{A43}$$

where a_ϵ^s and b_ϵ^s correspond to the annihilation operators of the fermion and anti-fermion, respectively. V is the volume of the system. Furthermore, in the presence of an external

magnetic field, we have

$$\int\int\frac{dp_1}{2\pi}\frac{dp_2}{2\pi}\longrightarrow\frac{eB}{2\pi}\sum_{n=0}^{\infty}. \tag{A44}$$

In the same way, we have

$$\begin{aligned}\hat{N} &= \int d^3x\bar{\psi}\gamma^0\psi\\ &= V\frac{eB}{2\pi}\sum_{n=0}^{\infty}\sum_{s=\pm1}\int\frac{dp_3}{2\pi}\Big(a_\epsilon^{s+}a_\epsilon^s-b_\epsilon^{s+}b_\epsilon^s\Big),\end{aligned} \tag{A45}$$

and

$$\begin{aligned}\hat{N}_5 &= \int d^3x\bar{\psi}\gamma^0\gamma^5\psi\\ &= V\frac{eB}{2\pi}\sum_{n=0}^{\infty}\sum_{s=\pm1}\int\frac{dp_3}{2\pi}\Big(\frac{s|\epsilon|}{E}a_\epsilon^{s+}a_\epsilon^s+\frac{s|\epsilon|}{E}b_\epsilon^{s+}b_\epsilon^s\Big),\end{aligned} \tag{A46}$$

Substituting Eqs. (A43) (A45) (A46) into Eq. (A1), after a simple calculation we obtain

$$\begin{aligned}\ln Z &= V\frac{eB}{2\pi}\sum_{n=0}^{\infty}\sum_{s=\pm1}\int\frac{dp_3}{2\pi}\Bigg(\frac{E}{T}+\ln\Big\{1+\exp\big[-(E-\mu\\ &\quad-\frac{s|\epsilon|}{E}\mu_5)/T\big]\Big\}+\ln\Big\{1+\exp\big[-(E+\mu-\frac{s|\epsilon|}{E}\mu_5)/T\big]\Big\}\Bigg).\end{aligned} \tag{A47}$$

Appendix B: Another approach with modified Lagrangian

In the Appendix A, we have derived the partition function of a fermion system with $\mathcal{P}$ violation and under a background magnetic field. We will discuss this subject in another approach in this appendix.

Absorbing the term including N_5 in Eq. (A1) into the Hamiltonian H, We can obtain the modified Lagrangian density

$$\mathcal{L}=\bar{\psi}(i\gamma^\mu D_\mu-m+\mu_5\gamma^0\gamma^5)\psi. \tag{B1}$$

Then the Dirac equation in Eq. (A6) is also modified as

$$i\partial_0\psi=\Big[(-i\partial_i-eA^i)\gamma^0\gamma^i+\gamma^0 m-\gamma^5\mu_5\Big]\psi. \tag{B2}$$

This Dirac equation can also be solved through the same method used in the above appendix, and here we just give the results. The wave function of the fermion is given as

$$u^s=\begin{pmatrix}\sqrt{E-(\epsilon-\mu_5)}\xi^s\\ \sqrt{E+(\epsilon-\mu_5)}\xi^s\end{pmatrix},\quad \text{with}\quad s=\pm1. \tag{B3}$$

When $n > 0$,

$$\xi^s = \frac{1}{\sqrt{2|\epsilon|}} \begin{pmatrix} (s)\mathrm{sgn}(p_3)\sqrt{|\epsilon| + s\lambda} \\ \sqrt{|\epsilon| - s\lambda} \end{pmatrix}, \quad \text{with} \quad \epsilon = s|\epsilon|; \tag{B4}$$

when $n = 0$,

$$\xi^1 = \begin{cases} (1,0)^T & \text{for} \quad p_3 > 0 \\ (0,1)^T & \text{for} \quad p_3 < 0 \end{cases}, \quad \text{with} \quad \epsilon = |p_3|, \tag{B5}$$

$$\xi^{-1} = \begin{cases} (0,1)^T & \text{for} \quad p_3 > 0 \\ (1,0)^T & \text{for} \quad p_3 < 0 \end{cases}, \quad \text{with} \quad \epsilon = -|p_3|. \tag{B6}$$

The wave function of the anti-fermion is

$$v^s = \begin{pmatrix} \sqrt{E - (\epsilon + \mu_5)}\xi^{-(s)} \\ -\sqrt{E + (\epsilon + \mu_5)}\xi^{-(s)} \end{pmatrix}, \quad \text{with} \quad s = \pm 1. \tag{B7}$$

When $n > 0$,

$$\xi^{-(s)} = \frac{1}{\sqrt{2|\epsilon|}} \begin{pmatrix} (-s)\mathrm{sgn}(p_3)\sqrt{|\epsilon| - s\lambda} \\ \sqrt{|\epsilon| + s\lambda} \end{pmatrix}, \quad \text{with} \quad \epsilon = -s|\epsilon|; \tag{B8}$$

when $n = 0$,

$$\xi^{-(1)} = \begin{cases} (0,1)^T & \text{for} \quad p_3 > 0 \\ (1,0)^T & \text{for} \quad p_3 < 0 \end{cases}, \quad \text{with} \quad \epsilon = -|p_3|, \tag{B9}$$

$$\xi^{-(-1)} = \begin{cases} (1,0)^T & \text{for} \quad p_3 > 0 \\ (0,1)^T & \text{for} \quad p_3 < 0 \end{cases}, \quad \text{with} \quad \epsilon = |p_3|. \tag{B10}$$

In the equations above, we have

$$\lambda = \sqrt{2neB}, \tag{B11}$$

$$|\epsilon| = \sqrt{\lambda^2 + p_3^2} = \sqrt{2neB + p_3^2}, \tag{B12}$$

$$E = \sqrt{(|\epsilon| - s\mu_5)^2 + m^2}. \tag{B13}$$

The partition function is given by

$$\begin{aligned} \ln Z = V\frac{eB}{2\pi}\sum_{n=0}^{\infty}\sum_{s=\pm 1}\int \frac{dp_3}{2\pi}\bigg(\frac{E}{T} + \ln\Big\{1 + \exp\big[-(E-\mu)/T\big]\Big\} \\ + \ln\Big\{1 + \exp\big[-(E+\mu)/T\big]\Big\}\bigg). \end{aligned} \tag{B14}$$

We should emphasize that the expression of particle energy E in the above equation is given by Eq. (B13).

In the same way, we can obtain

$$\begin{aligned}\hat{N}_5 &= \int d^3x\bar{\psi}\gamma^0\gamma^5\psi \\ &= V\frac{eB}{2\pi}\sum_{n=0}^{\infty}\sum_{s=\pm1}\int\frac{dp_3}{2\pi}\Big[\frac{(s|\epsilon|-\mu_5)}{E}a_\epsilon^{s+}a_\epsilon^s \\ &+\frac{(s|\epsilon|-\mu_5)}{E}b_\epsilon^{s+}b_\epsilon^s-\frac{(s|\epsilon|-\mu_5)}{E}\Big].\end{aligned}\tag{B15}$$

Making the ensemble average of $\hat{N}_5$ we have

$$\begin{aligned}N_5 &\equiv \langle\hat{N}_5\rangle \\ &= V\frac{eB}{2\pi}\sum_{n=0}^{\infty}\sum_{s=\pm1}\int\frac{dp_3}{2\pi}\Big[\frac{(s|\epsilon|-\mu_5)}{E}\frac{1}{e^{(E-\mu)/T}+1} \\ &+\frac{(s|\epsilon|-\mu_5)}{E}\frac{1}{e^{(E+\mu)/T}+1}-\frac{(s|\epsilon|-\mu_5)}{E}\Big].\end{aligned}\tag{B16}$$

N_5 can also been directly obtained through $N_5 = T\partial\ln Z/\partial\mu_5$.

Next, we calculate the chiral electric current density [15]:

$$\begin{aligned}\hat{j}_3 &= \frac{e}{V}\int d^3x\bar{\psi}\gamma^3\psi \\ &= \frac{e^2B}{2\pi}\sum_{n=0}^{\infty}\sum_{s=\pm1}\int\frac{dp_3}{2\pi}\Big[\big(\frac{s|\epsilon|-\mu_5}{E}\big)\big(\frac{sp_3}{|\epsilon|}\big)a_\epsilon^{s+}a_\epsilon^s \\ &-\big(\frac{s|\epsilon|-\mu_5}{E}\big)\big(\frac{sp_3}{|\epsilon|}\big)b_\epsilon^{s+}b_\epsilon^s+\big(\frac{s|\epsilon|-\mu_5}{E}\big)\big(\frac{sp_3}{|\epsilon|}\big)\Big].\end{aligned}\tag{B17}$$

Therefore, the ensemble average of $\hat{j}_3$ is

$$\begin{aligned}j_3 &\equiv \langle\hat{j}_3\rangle \\ &= \frac{e^2B}{2\pi}\sum_{n=0}^{\infty}\sum_{s=\pm1}\int\frac{dp_3}{2\pi}\Big[\big(\frac{s|\epsilon|-\mu_5}{E}\big)\big(\frac{sp_3}{|\epsilon|}\big)\frac{1}{e^{(E-\mu)/T}+1} \\ &-\big(\frac{s|\epsilon|-\mu_5}{E}\big)\big(\frac{sp_3}{|\epsilon|}\big)\frac{1}{e^{(E+\mu)/T}+1}+\big(\frac{s|\epsilon|-\mu_5}{E}\big)\big(\frac{sp_3}{|\epsilon|}\big)\Big].\end{aligned}\tag{B18}$$

Same as N_5, j_3 can also been obtained through

$$j_3 = -\frac{eT}{V}\Big(\frac{\partial\ln Z^+}{\partial p_3}-\frac{\partial\ln Z^-}{\partial p_3}\Big),\tag{B19}$$

where

$$\ln Z^+ = V\frac{eB}{2\pi}\sum_{n=0}^{\infty}\sum_{s=\pm1}\int\frac{dp_3}{2\pi}\ln\Big\{1+\exp\big[-(E-\mu)/T\big]\Big\},$$

and

$$\ln Z^- = V\frac{eB}{2\pi}\sum_{n=0}^{\infty}\sum_{s=\pm 1}\int\frac{dp_3}{2\pi}\Big(\frac{E}{T}+\ln\Big\{1+\exp\big[-(E+\mu)/T\big]\Big\}\Big), \tag{B20}$$

are the fermion part and anti-fermion part of the partition function in Eq. (B14), respectively. The minus related with the anti-fermion part in Eq. (B19) is due to our convention in Eq. (A12).

From Eq. (B18) we can find that only the states with $n = 0$ contribute to the chiral electric current density j_3, since the integral variable p_3 ranges from $-\infty$ to ∞ for $n > 0$, while from $-\infty$ to 0 or 0 to ∞ for $n = 0$. Therefor, j_3 can be simplified as

$$\begin{aligned} j_3 \;=\; & \frac{e^2B}{2\pi}\sum_{s=\pm 1}\int\frac{dp_3}{2\pi}\Big[\big(\frac{s|\epsilon|-\mu_5}{E}\big)\big(\frac{sp_3}{|\epsilon|}\big)\frac{1}{e^{(E-\mu)/T}+1} \\ & -\big(\frac{s|\epsilon|-\mu_5}{E}\big)\big(\frac{sp_3}{|\epsilon|}\big)\frac{1}{e^{(E+\mu)/T}+1}+\big(\frac{s|\epsilon|-\mu_5}{E}\big)\big(\frac{sp_3}{|\epsilon|}\big)\Big]. \end{aligned} \tag{B21}$$

In order to understand the physical meanings of the several terms in Eq. (B21), we just extract the term related with the positive fermion and calculate

$$\begin{aligned} & \sum_{s=\pm 1}\int dp_3\big(\frac{s|\epsilon|-\mu_5}{E}\big)\big(\frac{sp_3}{|\epsilon|}\big)\frac{1}{e^{(E-\mu)/T}+1} \\ = \; & \int_0^{\infty}dp_3\frac{p_3-\mu_5}{\sqrt{(p_3-\mu_5)^2+m^2}}\frac{1}{\exp[(\sqrt{(p_3-\mu_5)^2+m^2}-\mu)/T]+1} \\ & +\int_{-\infty}^{0}dp_3\frac{p_3-\mu_5}{\sqrt{(p_3-\mu_5)^2+m^2}}\frac{1}{\exp[(\sqrt{(p_3-\mu_5)^2+m^2}-\mu)/T]+1} \\ = \; & 0. \end{aligned} \tag{B22}$$

From the above equation we can find that, in the modified Lagrangian approach, it is $p_3 - \mu_5$ not p_3 that judges whether a particle is right-handed or left-handed, i.e., if the sign of $p_3-\mu_5$ is same as that of the particle spin along the z-direction, the particle is right-hand; if opposite, then the particle is left-hand. However, the direction of motion of the particle is governed by p_3 not $p_3 - \mu_5$. Therefore, the properties of right-handed or left-handed of a particle cannot determine the direction of motion of the particle. In another word, the left-right asymmetry cannot be correctly related with charge separation effect in this approach. So, we conclude that the modified Lagrangian approach is inappropriate to describe the chiral magnetic effect. We should point out that the approach given in Appendix A does not have this problem.

Next, we continue to calculate the chiral electric current density j_3 in Eq. (B21). The only nonvanishing contribution to j_3 come from the last term in Eq. (B21), i.e.

$$
\begin{aligned}
j_3 &= \frac{e^2B}{(2\pi)^2}\sum_{s=\pm1}\int dp_3\Big(\frac{s|\epsilon|-\mu_5}{E}\Big)\Big(\frac{sp_3}{|\epsilon|}\Big) \\
&= \frac{e^2B}{(2\pi)^2}\int_{-\infty}^{\infty} dp_3\frac{p_3+\mu_5}{\sqrt{(p_3+\mu_5)^2+m^2}} \\
&= \frac{e^2B}{(2\pi)^2}\int_{-\Lambda}^{\Lambda} dp_3\frac{p_3+\mu_5}{\sqrt{(p_3+\mu_5)^2+m^2}}\Big|_{\lim\Lambda\to\infty} \\
&= \frac{e^2B\mu_5}{2\pi^2}
\end{aligned}
\tag{B23}
$$

This is the result obtained in Ref. [15]. From our calculations above, one can find that j_3 calculated in the modified Lagrangian approach does not comes from the finite temperature contributions, however its source is the Dirac Sea which can be clearly seen in Eq. (B17). Therefore, it is argued in Ref. [15] that j_3 is independent of the temperature, chemical potential μ, and even the mass of the particle (from the calculations above we find that the independence of j_3 on the mass of the particle is due to the fact that the ultraviolet momentum in the Dirac Sea makes the mass of particle meaningless). We should comment that the results obtained in the modified Lagrangian approach are contrary to our physical intuition. On the one hand, the physical observable (here is the j_3) is unlikely to come from the Dirac sea. On the other hand, the chiral electric current density is also unlikely to be independent of the properties of current carriers. In this work we will show that the chiral electric density j_3 calculated in an appropriate approach, i.e., the approach in Appendix A, comes from the finite temperature contributions not the Dirac Sea, and j_3 is also dependent of the properties of current carriers and is also influenced by the external environment.

---

[1] I. Arsene *et al*, Nucl. Phys. **A 757**, 1 (2005).

[2] B. B. Back *et al*, Nucl. Phys. **A 757**, 28 (2005).

[3] J. Adams *et al*, Nucl. Phys. **A 757**, 102 (2005).

[4] K. Adcox *et al*, Nucl. Phys. **A 757**, 184 (2005).

[5] E. V. Shuryak, Prog. Part. Nucl. Phys. **53**, 273 (2004).

[6] F. Weber, Prog. Part. Nucl. Phys. **54**, 193 (2005).

[7] M. Alford, A. Schmitt, K. Rajagopal, and T. Schäfer, Rev. Mod. Phys. **80**, 1455 (2008).

[8] W. J. Fu, H. Q. Wei, and Y. X. Liu, Phys. Rev. Lett. **101**, 181102 (2008).

[9] B. I. Abelev *et al*, Phys. Rev. Lett. **103**, 251601 (2009).

[10] B. I. Abelev *et al*, arXiv:0909.1717 [nucl-ex].

[11] D. Kharzeev, Phys. Lett. **B 633**, 260 (2006).

[12] D. E. Kharzeev, L. D. McLerran, and H. J. Warringa, Nucl. Phys. **A 803**, 227 (2008).

[13] A. A. Belavin, A. M. Polyakov, A. S. Shvarts and Yu. S. Tyupkin, Phys. Lett. **B 59**, 85 (1975).

[14] S. L. Adler, Phys. Rev. **177**, 2426 (1969); J. S. Bell, and R. Jackiw, Nuovo Cim. **A 60**, 47 (1969).

[15] K. Fukushima, D. E. Kharzeev, and H. J. Warringa, Phys. Rev. **D 78**, 074033 (2008).

[16] D. E. Kharzeev and H. J. Warringa, Phys. Rev. **D 80**, 034028(2009).

[17] D. E. Kharzeev, Annals. Phys. **325**, 205 (2010).

[18] K. Fukushima, D. E. Kharzeev, and H. J. Warringa, arXiv:0912.2961 [hep-ph].

[19] M. Abramczyk, T. Blum, G. Petropoulos, and R. Zhou, arXiv:0911.1348 [hep-lat].

[20] M. Asakawa, A. Majumder, and B. Müller, arXiv:1003.2436 [hep-ph].

[21] W. J. Fu, Y. X. Liu, and Y. L. Wu, arXiv:1002.0418 [hep-ph].

[22] C. Ratti, M. A. Thaler, and W. Weise, Phys. Rev. **D 73**, 014019 (2006).

[23] S. Rößner, C. Ratti, and W. Weise, Phys. Rev. **D 75**, 034007 (2007).

[24] S. K. Ghosh, T. K. Mukherjee, M. G. Mustafa, and R. Ray, Phys. Rev. **D 73**, 114007 (2006); S. Mukherjee, M. G. Mustafa, and R. Ray, Phys. Rev. **D 75**, 094015 (2007)

[25] W. J. Fu, Z. Zhang, and Y. X. Liu, Phys. Rev. **D 77**, 014006 (2008).

[26] W. J. Fu, Y. X. Liu, and Y. L. Wu, Phys. Rev. **D 81**, 014028 (2010).

[27] P. Rehberg, S. P. Klevansky, and J. Hüfner, Phys. Rev. **C 53**, 410 (1996).

[28] S. A. Voloshin, Phys. Rev. **C 70**, 057901 (2004).

[29] Y. L. Ma, and Y. L. Wu, Int. J. Mod. Phys. **A 21**, 6383 (2006).

[30] M. A. Metlitski, and A. R. Zhitnitsky, Phys. Rev. **D 72**, 045011 (2005).

[31] J. Ambjorn, J. Greensite and C. Peterson, Nucl. Phys. **B 221**, 381 (1983).